Available online at www.sciencedirect.com
ScienceDirect
International Journal of Mass Spectrometry 262 (2007) 241–246
International Journal of Mass Spectrometry
www.elsevier.com/locate/ijms

Calibration of a quadrupole ion trap for particle mass spectrometry

Adam J. Trevitt, Philip J. Wearne, Evan J. Bieske*

School of Chemistry, University of Melbourne, Vic. 3010, Australia

Received 10 November 2006; received in revised form 30 November 2006; accepted 30 November 2006
Available online 12 January 2007

Abstract

A quadrupole ion trap (QIT) is calibrated for microparticle mass spectrometry by confining $\phi = 2.02$ μm dye-labeled polystyrene microspheres and measuring their secular oscillation frequencies and fluorescence spectra. A particle's absolute mass and charge are found by measuring its secular oscillation frequencies within the QIT while initiating charge steps through photo-ejection of electrons. The radius of the same microsphere is determined by analyzing the fluorescence emission spectrum, which is dominated by optical cavity resonances, employing Mie theory. The mass of the microsphere is calculated from the radius using the density of bulk polystyrene. For nine particles originating from the same stock sample, the masses obtained from the two methods agrees to within 3% with no systematic deviation. Analysis reveals that small uncertainties in the secular frequency measurements result in significant error in the absolute charges and masses. Nevertheless, excellent agreement between the average masses determined using the two techniques confirm that the value of the trap parameter (z_0) obtained from computer modeling is appropriate and that effects of electrode misalignments are small.

PACS: 07.75.+h; 78.66.Vs; 39.10.+j; 42.25.Fx

Keywords: Quadrupole ion trap; Microparticle; Optical resonance; Mie scattering

1. Introduction

Accurate mass determination for particles in the 10–10,000 nm size regime is desirable to characterize atmospheric aerosols, viruses, bacteria and advanced particulate materials. However, particles in this size range are usually too large for conventional mass spectrometers yet too small for conventional mass balances. There have been several efforts towards developing techniques for the non-destructive mass spectrometric characterization of single particles, particularly in quadrupole ion traps (QITs) [1]. The foundations of single microparticle QIT mass spectrometry (QIT-MS) were established by Wuerker et al. who demonstrated that the mass-to-charge ratio (m/Q) of a single trapped particle can be determined from its secular oscillation frequencies in a QIT [2]. Subsequently, several groups have applied this strategy to single microparticle mass measurements [3–6], culminating in the work of Peng et al. who determined the masses of individual biological microparticles including *Escherichia coli* and human red blood cells [7,8].

One outstanding problem for single microparticle QIT-MS involves mass calibration of the device for operation in the high mass regime. In principle, once the electrode spacing is known, the mass-to-charge ratio of a charged particle in an ideal Paul trap with infinite hyperbolic electrodes can be ascertained from its secular oscillation frequencies. However, practical traps have electrodes that are non-ideal and which may be misaligned. As pointed out by Schlemmer et al. [5] electrode imperfections and misalignments on the order of tens of microns can lead to systematic errors in m/Q measurements in the percent range.

A recently reported calibration procedure involved mass analysis of single 0.895 μm diameter polystyrene microparticles originating from a highly monodisperse stock sample [9]. The method entailed visually monitoring star oscillation trajectories and initiating charge steps using electron impact to obtain the particle's absolute charge and mass. Measured particle masses agreed very well with masses deduced from size and density data specified by the particles' supplier. One disadvantage of the method is that it relies on size data from the manufacturer. A more desirable procedure would involve ascertaining the size and mass of the same particle in situ. This was attempted some time ago by Davis and Ray [10], who measured the size and mass for a single microsphere ($\phi = 2$ μm) using an electrodynamic

* Corresponding author. Tel. +61 3 8344 7082; fax: +61 3 9347 5180.
E-mail address: evanjb@unimelb.edu.au (E.J. Bieske).

1387-3806/$ – see front matter © 2007 Elsevier B.V. All rights reserved.
doi:10.1016/j.ijms.2006.11.019

balance (EDB). The particle's size was obtained from analysis of the angle dependent elastic light scattering and its mass from the electric field required to balance the particle at the EDB centre. Radii deduced using the two methods agreed to within 20%. Recently, Zheng et al. improved this procedure for larger microspheres ($\phi = 21$ μm) in an EDB, with radii determined through spring point, aerodynamic drag and light scattering measurements agreeing to within 3.9% [11].

In the current work, we characterize single, $\phi = 2.02$ μm dye-labeled polystyrene microparticles (4.5×10^{-15} kg, 2.7×10^{12} Da) by obtaining their cavity enhanced fluorescence spectra, and by measuring their secular oscillation frequencies in the QIT. Analysis of optical morphology dependent resonances (MDRs) of a single microsphere allowed the particle's radius to be determined, and thenceforth for its mass to be ascertained [12]. The m/Q of the same microparticle was measured from observation of its secular frequency in the trap. In turn, by initiating single electron charge steps the particle's absolute charge and mass were determined. Following a discussion of both techniques, we present data for nine particles, and finally discuss sources of error in the mass determinations.

2. Experimental methods

2.1. Materials

The fluorescent polystyrene microparticles used in this study were commercially obtained as an aqueous suspension (Duke Scientific, nominal diameter ~ 2 μm). Each particle contains fluorescent dye molecules (MW = 200–300 Da) incorporated into the polystyrene matrix. The particles have a broad absorption peaking at 412 nm and an emission envelope extending over 440–550 nm with broad peaks at 445 and 473 nm. The manufacturer's quoted density for the particles is 1.05 g/cm^3, which corresponds to the density of bulk polystyrene.

2.2. The quadrupole ion trap

The quadrupole ion trap (QIT) used in this work follows the design of Schlemmer et al. [5] consisting of two opposing conical "endcap" electrodes surrounded by eight rod electrodes, which replace the ring electrode of a conventional Paul trap (see Fig. 1). This electrode geometry generates an approximate quadrupole potential in a small volume around the trap centre while having the advantage of excellent optical access to the trapped particle [13]. The QIT was housed in a UHV chamber (Fig. 2) evacuated by a 170 L/s turbo pump. The secular frequencies of a single particle were measured at a pressure of ~ 10^{-6} Torr. Fluorescence spectra were obtained in the presence of helium buffer gas (50 mTorr) to reduce the particle's oscillation amplitude.

2.3. Theoretical background

The equations describing the stability and motion of a charged particle in a quadrupole field are well known [14]. Here, we introduce only the equations relevant for determining the m/Q of a trapped particle from its frequency of motion [2,5]. The

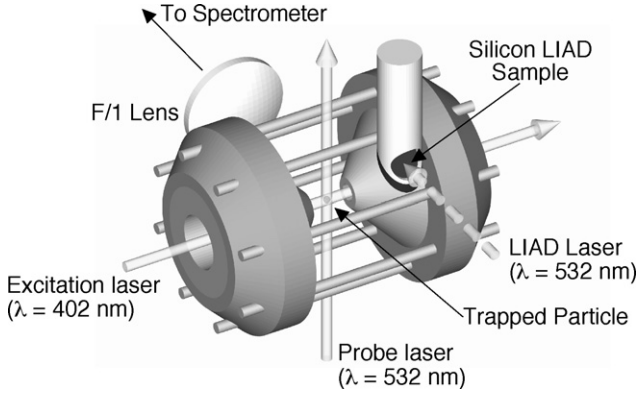

Fig. 1. View of the quadrupole ion trap (QIT).

stability parameters in the axial (z) and radial (r) directions for a QIT operated in single phase (oscillating potential applied to endcap electrodes and ring electrode held at ground) are:

$$q_z = -2q_r = \frac{2QV}{mz_0^2\Omega^2}, \tag{1}$$

where V is the amplitude of the oscillating voltage applied to the QIT endcap electrodes at an angular frequency of Ω. In an ideal QIT, z_0 is half the distance between the endcap electrodes. The potential distribution within the QIT was modeled using the simulation program SIMION 3D v7.0 (Idaho National Laboratories) with a resolution of 0.05 mm/gu over a 1 mm^3 cube. The quadrupole field near the trap centre was found to be consistent with $z_0 = 5.89$ mm.

A particle confined in an ideal Paul trap has secular frequencies in the radial (ω_r) and axial (ω_z) directions of:

$$\omega_z = 2\omega_r = \beta_z \frac{\Omega}{2} \tag{2}$$

where, for $q_z < 0.7$, the dependence of β_z on q_z is adequately approximated by

$$\beta_z = \left(\frac{q_z^2}{2 - q_z^2} - \frac{7}{128} q_z^4 + \frac{29}{2304} q_z^6 \right)^{1/2} \tag{3}$$

For the secular frequency measurements, q_z was maintained at ~ 0.3 by choosing appropriate values for V and Ω ($V \approx 1500$ V and $\Omega/2\pi \approx 350$ Hz). The m/Q value is obtained from ω_r through the inverse relation between q_z and β_z which was approximated as an 8th order polynomial.

The gravitational force perturbs the particle's motion splitting the doubly degenerate radial secular oscillation (ω_r) into vertical (ω_y) and horizontal (ω_x) components. To compensate for gravity and maintain the particle at the trap centre, a dc potential was applied between the vertically opposed pairs of rod electrodes. It has been shown that provided the particle is balanced at the trap center the secular frequencies correspond to those described by Eqs. (1)–(3) [5,13]. Note that as a consequence of the probe laser orientation only ω_x and ω_z were measured in this work (see Fig. 1).

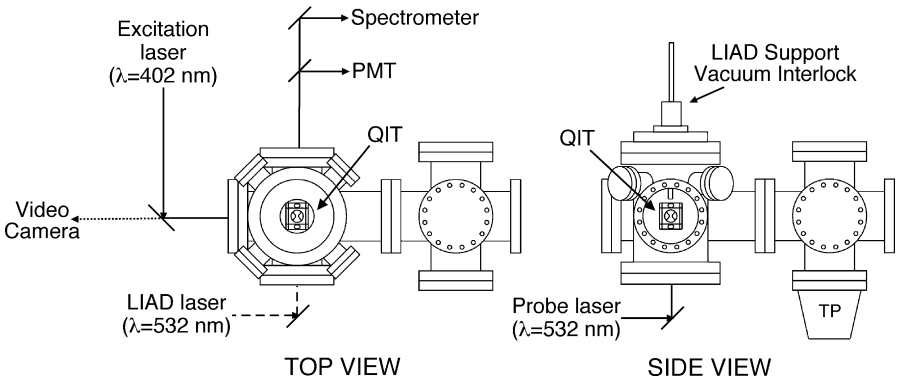

Fig. 2. View of the experimental set-up.

2.4. Optical set-up

For the secular frequency measurements, the gently focussed output of a continuous wave Nd:YVO_4 laser ($\lambda = 532$ nm, Coherent VERDI-V5) was aligned through the QIT centre (Fig. 1). Elastically scattered 532 nm light was collected by a 25 mm F/1 lens and directed to a photomultiplier tube (PMT) (Hamamatsu H5784-02) through a spatial filter. The signal from the PMT was filtered using a low-pass Butterworth frequency filter (Krohn-Hite 3381) to remove high frequency components. The filtered signal was sent to a personal computer via a data acquisition card (NI PCI-6024E). The time domain signal was Fourier transformed (FT) to ascertain the particle's secular oscillation frequencies. During a frequency measurement, the particle was monitored using a video camera and its oscillation amplitude was maintained at 150 ± 20 μm. Each frequency measurement entailed collection of 40,000 sample points at a collection rate of 200 Hz, corresponding to a frequency resolution of 0.005 Hz.

For fluorescence measurements, the particles were irradiated by the $\lambda = 402$ nm frequency doubled output from a picosecond Ti:Sapphire laser (Tiger-ps, Time-Bandwidth). The light was directed through the QIT via holes in the endcap electrodes (Fig. 1). Fluorescence from the particle was collected by a 25 mm F/1 lens and directed into a spectrometer (JY Triax 552) with a liquid nitrogen cooled CCD detector (JY Symphony) and 600 g/mm grating. The spectral resolution was ~0.05 nm. The spectrometer was regularly calibrated using a HgAr lamp.

2.5. Particle injection and single particle isolation

Polystyrene particles were introducted into the QIT using laser induced acoustic desorption (LIAD) [8,9]. Preparing a LIAD sample involved placing two to three drops of a purified aqueous particle suspension on a 0.5 mm thick Si wafer which was then dried under nitrogen. The wafer was held above the QIT by a stainless steel rod that was inserted into the vacuum chamber through a vacuum interlock (Fig. 1). A single focussed 7 ns laser pulse ($\lambda = 532$ nm, ~40 mJ) from a Q-switch Nd:YAG laser irradiated the Si wafer from behind causing charged particles to be desorbed from the front surface. Helium buffer gas (50 mTorr) slowed the desorbed particles so that they could be trapped efficiently.

Several methods were used to check that only one particle was confined in the QIT. The presence of broadened or additional peaks in the FT spectrum usually indicated the presence of more than one particle. Additionally, when inspected with a video camera, a lone particle had a smooth periodic trajectory, whereas irregularities in the particle's motion usually implied presence of one or more additional intruding particles (not necessarily illuminated by the probe laser). Once unwanted particles were ejected (by systematically varying V and/or Ω), the remaining particle adopted a smooth, periodic trajectory.

2.6. Charge stepping

The absolute charge and mass of each particle were determined by measuring ω_x for a number of different charge states which could be converted to m/Q values using Eqs. (1)–(3).

Charge stepping of single polystyrene microparticles was accomplished using the output from a pulsed Xe flashlamp (Ocean Optics PX-2, $\lambda = 220$–750 nm) transmitted to the trap through a UV-grade optical fibre. Two processes were presumably responsible for charge changing events. First of all, the particles could lose electrons through direct photo-ejection caused by photons with $\lambda < 294$ nm, whose energy exceeded the polystyrene work function (4.22 eV [15]). Alternatively, electrons photo-ejected from the metal electrodes may have been accelerated into the trap centre where they were either absorbed by the particle or induced secondary electron ejection. Often the flashlamp was fired >100 times before a change of one or several elementary charge units was observed.

For highly charged particles, it was difficult to discern quickly whether a small charge change had occurred after irradiation. A simple and rapid technique was to view *star* trajectories which are present at certain trap drive frequencies [4,7]. A single trapped particle adopts a stable star trajectory in the x–y plane with n branches when the drive frequency (Ω) is equal to an integer multiple of the particle's radial frequency ($n\omega_r$). Two examples of star trajectories are shown in Fig. 3. Usually, to detect small charge changes on highly charged microparticles ($Q > 400e$), a stable star pattern trajectory was established (with $n = 6$ or 7) by carefully adjusting the drive frequency while viewing the particle using a video camera. Once a stationary star trajectory was established, the Xe flashlamp was

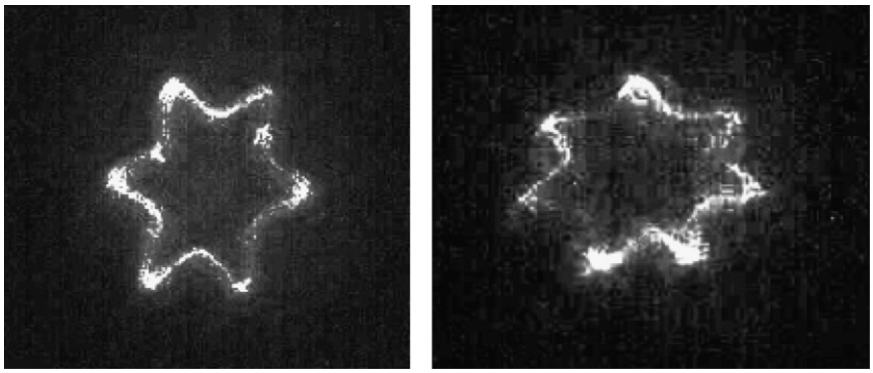

Fig. 3. Star trajectories in the x-y plane for a trapped polystyrene microparticle with $n = 6$ (left) and $n = 7$ (right).

pulsed. When a charge step occurred, the star pattern began to rotate slowly because the drive frequency was no longer an integer multiple of the particle's secular frequency. Subsequently, the particle's new secular frequency was measured.

3. Results and discussion

The MDR dominated fluorescence emission from a single polystyrene microsphere is shown in Fig. 4. The MDR peaks are sharp and symmetric indicating that the particle has high sphericity [16]. Furthermore, the MDR spacing reveals that the particle is a single sphere rather than a bisphere or agglomerate. The particle's radius and refractive index were determined from an analysis of the MDR wavelengths [12] and found to be consistent with a sphere of radius $a = 1010 \pm 1$ nm and refractive index $m_\lambda = 1.551 + 11430\,\text{nm}^2/\lambda^2$. The calculated Mie scattering spectrum for a sphere with the fitted parameters is also shown in Fig. 4. Clearly, the match between theory and experiment is excellent. Using the bulk polystyrene density (1.05 g/cm^3), the particle was calculated to have a mass $m_{\text{MDR}} = 4.54 \times 10^{-15}$ kg. Note that polystyrene has been shown to have a density close to that of the bulk for structures down to nanometer scales [17].

The m/Q of the same microsphere was determined by measuring its horizontal secular frequency (ω_x) and using Eqs. (1)–(3). A typical FT spectrum is shown in Fig. 5, where ω_x is identified. The particle's absolute charge and mass were ascertained by initiating charge steps using the Xe flashlamp. In this case, ω_x for the particle was measured for eight charge states (Fig. 6a).

Determination of a particle's absolute mass (m_{FT}) and charge ($Q = Ze$, where Z is an integer) was achieved by the procedure described in references [9] and [18]. In the first step, a series of charge assignments (Z_i) were made for the eight Q/m states. This was done by assigning a Z value to the first Q/m state and using the ratio of Q/m values to make Z assignments for the other states. Next, the corresponding masses for the eight Q/m states were calculated, along with the average mass and its standard deviation. This procedure was repeated by varying the initial integer charge state assignment Z_1 from 1 to 2000 to ascertain the set of charge states that yielded the average mass with the lowest standard deviation. The outcome is conveniently represented as a plot of standard deviation (σ) versus m_{FT}, in which the mass corresponding to the best charge state assignments can be identified (Fig. 6b). The result for the data shown in Fig. 6 is m_{FT}=4.72×10^{-15} kg, which is ∼4% larger than $m_{\text{MDR}} = 4.54 \times 10^{-15}$ kg.

Nine microspheres from the same stock sample were investigated using the procedure outlined above to determine a series of m_{FT} and m_{MDR} values. From the fluorescence spectra, it was found that the particles' radii varied from 1002.7 to 1013.8 nm with an average value $\bar{a} = 1011.1 \pm 2.2$ nm. The standard deviation of a (≈0.2%) is considerably less than the manufacturer's specified tolerance (1.5%). The value of $\bar{a}$ corresponds to an average mass $\bar{m}_{\text{MDR}} = 4.55 \pm 0.03 \times 10^{-15}$ kg, which compares very well with the average mass determined

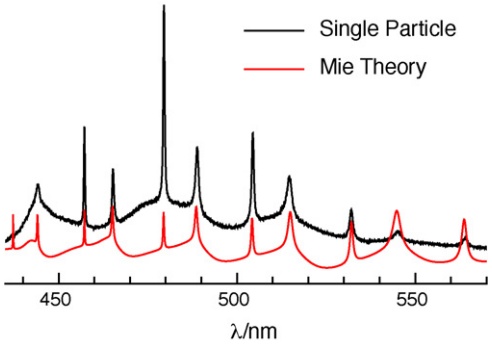

Fig. 4. Fluorescence emission spectra from a single microsphere (upper) and the calculated scattering spectrum (lower) for fitted parameters of $a = 1010$ nm and $m_\lambda = 1.551 + 11430\,\text{nm}^2/\lambda^2$.

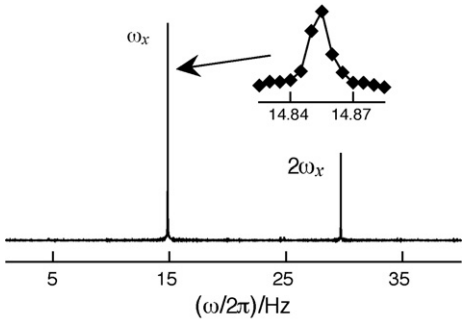

Fig. 5. Frequency spectrum for a single polystyrene particle confined in the QIT with $V_{0-p} = 1500$ V, $\Omega/2\pi = 350$ Hz. The strongest peak corresponds to oscillation in the x direction (ω_x) while the weaker peak is its harmonic ($2\omega_x$).

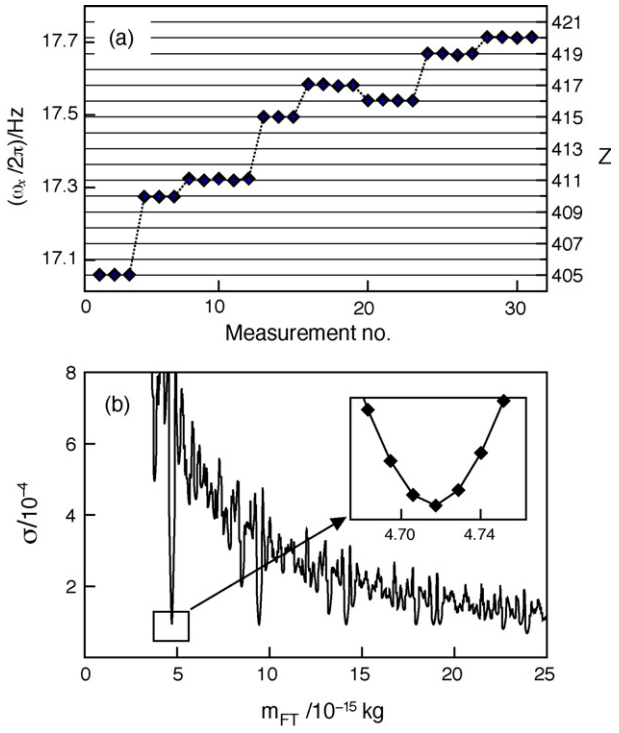

Fig. 6. (a) Plot of a single particle's oscillation frequency. Frequency steps correspond to charge changes initiated by the Xe flashlamp. Trap parameters ($V_{0-p} = 750$ V and $\Omega/2\pi = 330$ Hz) were kept constant throughout. The right-hand axis gives the particle's absolute charge number (Z). Also shown (b) is a plot of the standard deviation (σ) for masses corresponding to a range of charge assignments The lowest σ corresponds to $m_{FT} = 4.72 \times 10^{-15}$ kg.

from the Q/m and charge stepping measurements ($\bar{m}_{FT} = 4.54 \pm 0.12 \times 10^{-15}$ kg).

The m_{MDR} values are plotted against the m_{FT} values for the nine particles in Fig. 7. Fitting the data to a straight line yields $m_{MDR} = (1.002 \pm 0010) \times m_{FT}$. The excellent correlation between m_{FT} and m_{MDR} suggests that the trap parameter $z_0 = 5.89$ mm determined from the computer simulations is indeed appropriate, and that the effect of any electrode misalignment is small.

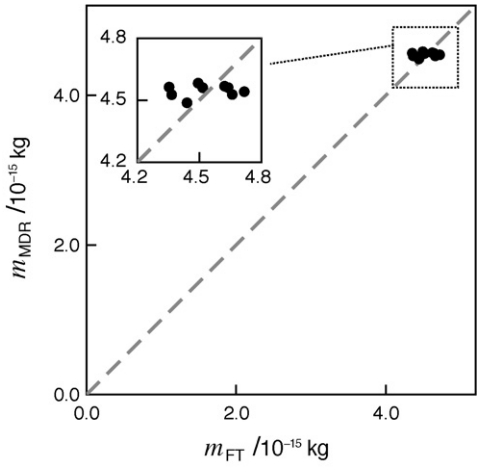

Fig. 7. Mass determined from the MDR analysis (m_{MDR}) plotted against mass obtained from secular frequency measurements (m_{FT}).

There is the possibility that the density of the polystyrene sphere differs slightly from the bulk value because of the incorporation of the dye molecules. If this was the case, the m_{MDR} values would be systematically too high or too low. However, one might expect that significant changes in the density would be reflected in changes in the material's refractive index. The average refractive index value determined from the Mie analysis for the nine particles is 1.583 ± 0.006 at 589 nm, very close to the reported refractive index of polystyrene (1.59 at 589 nm; Ref. [19]), suggesting that, despite being impregnated with fluorescent molecules, the density of the microspheres is very similar to that of bulk polystyrene. Furthermore, we observe no correlation between m_{FT} or m_{MDR} and the refractive index values, which, if present, would imply particle-to-particle density variations.

It is apparent from Fig. 7 that the range of the m_{FT} data is ~4 times larger than that of the m_{MDR} data. Obviously, the m_{FT} spread primarily reflects the uncertainty in the m_{FT} measurements rather than resulting from a range of particle sizes, otherwise m_{MDR} and m_{FT} would have similar spreads.

The main random error in m_{FT} is likely to arise from the uncertainty in the absolute charge state assignment which originates from the uncertainty in the Q/m values. The precision of the Q/m determination is governed by errors in ω, Ω and V (see Eq. (1)). We estimate that the relative errors in in ω_x, Ω and V are of the order of 3.3×10^{-4}, 1×10^{-5} and 1×10^{-3}, respectively.

Because Ω and V are fixed during a charge stepping experiment, it is likely that the Q and m_{FT} determinations are affected mainly by random errors in the ω_x measurements. To systematically explore the relationship between errors in ω_x and in the resulting charge (Q) and mass (m_{FT}) values, we ran a series of simulations on model data for a 2.02 μm polystyrene sphere. To begin with, the particle was assumed to have undergone a series of seven charge steps corresponding to charge numbers of 450, 453, 454, 456, 457, 458, 461 and 463, which are typical Z values for the particles characterized in this work. The corresponding ω_x values were calculated using Eqs. (1)–(3). These ω_x values were then varied randomly over a range determined by an assumed relative error ($\Delta\omega_x/\omega_x$). The charge and mass assignment procedure outlined above was then performed using the noisy ω_x values to recover the particle's mass and charge states which, because of the introduced random errors, did not necessarily correspond with the initial assumed charges. For each assumed relative error in ω_x, this process was repeated 1500 times to gain a statistically significant estimate of the uncertainty in the charge (Z and Q) and mass (m_{FT}).

The results of the simulations are displayed in Fig. 8, where the relative uncertainty in the charge state assignment ($\Delta Z/Z$) is plotted against the relative error in ω_x. It is evident that relatively small fractional errors in ω_x lead to much larger relative errors in the absolute charge number (Z) and consequently in the absolute mass (m_{FT}).

It is clear from the simulations that, for example, errors in the ω_x frequency measurements on the order of the experimental frequency resolution (0.005 Hz, corresponding to a fractional error of 3.3×10^{-4}), leads to uncertainties in the charge and mass of 1–2%, comparable with the observed 2.6% spread in the m_{FT}

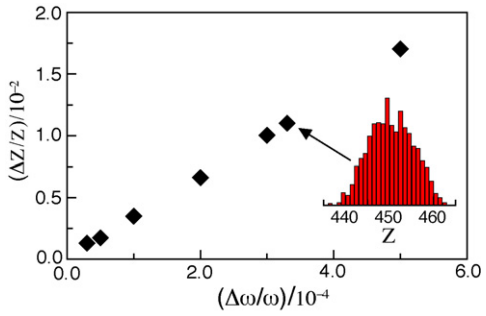

Fig. 8. Relative error in the charge state assignment $\Delta Z/Z$ plotted against the relative error in the secular frequency measurement $\Delta\omega/\omega$. The histogram shows the distribution of charge states (Z) arising from a relative error in ω_x of 3.3×10^{-4}.

values for the nine particles. The fluctuations in Ω and V during a series of secular frequency measurements should be much less than their absolute uncertainties (and to the uncertainty in ω_x) and therefore are not expected to contribute significantly to the precision of Q. They may, however, have a small effect on the overall accuracy of m_{FT}. The presence of surface charges on the electrodes may also have an effect on the measured ω_x values, thereby influencing the accuracy and precision of the m_{FT} determinations. In this regard, it is worth recalling that the charge state changes were effected by UV light from a pulsed Xe lamp, a fraction of which would have inevitably impinged on the electrode surfaces. While it is difficult to quantify the surface charge effects, they may account for part of the 2.6% spread in the m_{FT} data for the nine particles.

There are several improvements that could be made in the mass calibration procedure, particularly relating to the determination of the particles' absolute mass and charge from measurements of their secular frequencies in the trap. Most significantly, the m/Q determinations would be more accurate for smaller particles with lower charges for which an incremental charge change would lead to a larger frequency shift. The difficulty is that a smaller particle would exhibit fewer MDR's in the range of the dye emission profile, reducing the accuracy of the radius determined from the Mie analysis. However, this limitation could be overcome by using UV light to irradiate particles doped with appropriate fluorophores and monitoring emission in the 300–400 nm range.

4. Summary

A calibration procedure for a microparticle QIT-MS is described. The procedure combines MDR enhanced fluorescence spectroscopy with single particle frequency measurements and charge stepping. The average masses obtained for nine particles using each technique are in excellent agreement ($\bar{m}_{MDR} = 4.55 \pm 0.03 \times 10^{-15}$ kg and $\bar{m}_{FT} = 4.54 \pm 0.12 \times 10^{-15}$ kg). This suggests that the trap geometrical parameter ($z_0 = 5.89$ mm) obtained by computer simulation is appropriate. The large relative errors of the absolute charges and masses determined from secular frequency measurements could be reduced in the future by studying smaller particles.

Acknowledgments

The Australian Research Council and University of Melbourne are acknowledged for financial support. We thank R. J. Mathys for outstanding technical assistance and R. Crowe and C. Turner for assistance in acquiring data. We also thank Drs. H.-C. Chang and W.-P. Peng (IAMS Taiwan) for helpful discussions.

References

[1] W.-P. Peng, Y. Cai, H.-C. Chang, Mass Spec. Rev. 23 (2004) 443.
[2] R.F. Wuerker, H. Shelton, R.V. Langmuir, J. Appl. Phys. 30 (1959) 342.
[3] H. Winter, H.W. Ortjohann, J. Am. Phys. 59 (1991) 807.
[4] G. Hars, Z. Tass, J. Appl. Phys. 77 (1995) 4245.
[5] S. Schlemmer, J. Illemann, S. Wellert, D. Gerlich, J. Appl. Phys. 90 (2001) 5410.
[6] S. Schlemmer, S. Wellert, F. Windisch, M. Grimm, S. Barth, D. Gerlich, Appl. Phys. A 78 (2004) 629.
[7] W.-P. Peng, Y.-C. Chang, M.-W. Kang, Y.T. Lee, H.-C. Chang, J. Am. Chem. Soc. 126 (2004) 11766.
[8] W.-P. Peng, Y.-C. Chang, M.-W. Kang, Y.-K. Tzeng, Z. Nie, H.-C. Chang, C.-H. Chen, Angew. Chem. Int. Ed. 45 (2006) 1423.
[9] W.-P. Peng, Y.-C. Chang, C.-W. Lin, H.-C. Chang, Anal. Chem. 77 (2005) 7084.
[10] E.J. Davis, A.K. Ray, J. Colloid Interface Sci. 75 (1980) 566.
[11] F. Zheng, M.L. Laucks, E.J. Davis, J. Aerosol Sci. 31 (2000) 1173.
[12] J.D. Eversole, H.-B. Lin, A.L. Huston, A.J. Campillo, P.T. Leung, S.Y. Liu, K. Young, J. Opt. Soc. Am. B 10 (1993) 1955.
[13] J. Illemann, Ph.D. Thesis, TU Chemnitz, 2000, URL: http://archiv.tu-chemnitz.de/pub/2000/0067.
[14] P.H. Dawson (Ed.), Quadrupole Mass Spectrometry and its Applications, Elsevier Scientific Publishing Co., Amsterdam, 1976;
R.E. March, R.J. Hughes, Quadrupole Storage Mass Sprectrometry, Wiley, New York, 1989;
R.E. March, J.F.J. Todd (Eds.), Fundamentals of Ion Trap Mass Spectrometry, vol. 1 of Practical Aspects of Ion Trap Mass Spectrometry, CRC Press, Inc., 1995.
[15] D.K. Davies, J. Phys. D 2 (1969) 1533.
[16] A.J. Trevitt, P.J. Wearne, E.J. Bieske, M.D. Schuder, Opt. Lett. 31 (2006) 2211.
[17] W.E. Wallace, N.C. Beck Tan, W.L. Wu, S. Satija, J. Chem. Phys. 108 (1998) 3798.
[18] M.A. Tito, K. Tars, K. Valegard, J. Hajdu, C.V. Robinson, J. Am. Chem. Soc. 122 (2000) 3550.
[19] Duke Scientific Co. Technical Note 007B, http://www.dukescientific.com/pdfs/tech/Tn00702Web.pdf.